RSC Advances

PAPER

View Article Online
View Journal | View Issue

Cite this: *RSC Adv.*, 2024, **14**, 27565

Porous carbon/Fe_3O_4 nanocomposite as a new magnetically recoverable catalyst for the preparation of polyhydroquinolines†

Hamid Goudarziafshar,*[a] Maryam Zafari[a] and Ahmad Reza Moosavi-Zare *[ab]

Received 26th July 2024
Accepted 15th August 2024

DOI: 10.1039/d4ra05432f

rsc.li/rsc-advances

A porous carbon/Fe_3O_4 nanocomposite (PC/Fe_3O_4 nanocomposite) was prepared through the pyrolysis of peanut shells as biowaste with ferrous ferric oxide to give a new magnetically recoverable catalyst. In the designed nanocomposite, magnetic iron oxide nanoparticles are properly distributed on the surface and cavities of porous carbon obtained from biomass. Increasing the active surface and magnetic recovery capability results in catalytic synergy, thereby promoting the reaction with an appropriate catalytic effect. The catalytic ability of the porous carbon/Fe_3O_4 nanocomposite as a nanomagnetically recoverable catalyst was successfully tested for the synthesis of polyhydroquinolines.

1. Introduction

1,4-Dihydropyridine derivatives exhibit important medicinal properties, such as antimalarial, antiasthmatic, anti-inflammatory, anticancer, antimicrobial, antioxidant and antibacterial activities.[1–5] Moreover, these materials have been used as tyrosine kinase inhibiting materials.[6] Polyhydroquinoline compounds, containing a 1,4-dihydropyridine ring in their structure, show some significant pharmacological properties, including antiatherosclerotic, antitumour, geroprotective, vasodilator, bronchodilator and hepatoprotective activity.[7]

The multi-component synthesis of polyhydroquinolines *via* the reaction of arylaldehydes, dimedone (5,5-dimethylcyclohexane-1,3-dione), β-ketoesters and ammonium acetate is one of the most important protocols for the synthesis of these important compounds.[8] High yield of products, short reaction times, saving energy and starting materials, as well as producing the final product in shorter steps are some advantages of this protocole.[9–17]

The multicomponent preparation of polyhydroquinoline derivatives has been reported using various catalysts, such as Cu-IRMOF-3,[8] nano-Fe_3O_4,[18] sulfonic acid functionalized pyridinium chloride,[19] nano-[Mn-4NSMP]Cl_2,[20] silica-bonded imidazolium-sulfonic acid chloride,[21] nano-[Fe-PSMP]Cl_2,[22] nano-$CoAl_2O_4$,[23] Cu(II)@PHQSS,[24] $SnFe_2O_4$@SiO_2@SO_3H,[25] [pyridine-1-SO_3H-2-COOH]Cl,[26] Fe_3O_4@CQD@Si(OEt)$(CH_2)_3$NH@CC@Ad@Cu$(OAc)_2$,[27] nickel nanoparticles,[28] [NMP][HSO_4],[29] FeF_3,[30] and [Fe_3O_4@SiO_2/*N*-propyl-1-(thiophene-2-yl) ethanimine][$CoCl_2$].[31]

Owing to the low price, low density, biodegradability, good electrical conductivity and easy thermal decomposition, biomass waste can be reused as a renewable and degradable material.[32–36] Recently, agricultural waste has been used as one of the sources of biomass in the preparation and design of catalysts. One of these materials is peanut shells, which have been used as a suitable starting material in the production of porous carbon owing to their low density and high fiber content. Adding metal oxides and other functional groups to a porous carbon substrate with a high effective surface is the basis of designing new catalysts with high catalytic power and chemical activity in chemical reactions.[37]

Peanut shells as a biomass obtained from agricultural waste have been used in carrying out limited chemical processes, including the cycloaddition of epoxides by carbon dioxide,[37] decomposition of polluting organic compounds,[38] synthesis of aromatic rich monomers,[39] preparation of 5-hydroxymethylfurfural derivatives from polysaccharides and monosaccharides (such as cellulose, glucose, sucrose, and some agricultural wastes),[40] esterification of cyclohexene by formic acid,[41] and preparation of *H*-pyrimido[2,1-*b*] benzimidazoles[42] and 1,2,3-triazole compounds.[43]

Scientists and technologists have been drawn to magnetic nanoparticles owing to their important properties, including particle size, morphology, and magnetic activity. Magnetic nanoparticles have been widely used in the design of supported catalysts and the preparation of catalysts with a core–shell structure. The presence of these particles in the structure of a catalyst causes a simple separation of the catalyst from the reaction mixture *via* an external magnet, and it can be reused in other reactions. Furthermore, magnetic nanoparticles have

[a]*Department of Chemical Engineering, Hamedan University of Technology, Hamedan, 65155, Iran. E-mail: moosavizare@yahoo.com; hamid_gafshar@yahoo.com*

[b]*Chemistry Department, College of Sciences, Shiraz University, Shiraz 71946-84795, Iran*

† Electronic supplementary information (ESI) available. See DOI: https://doi.org/10.1039/d4ra05432f

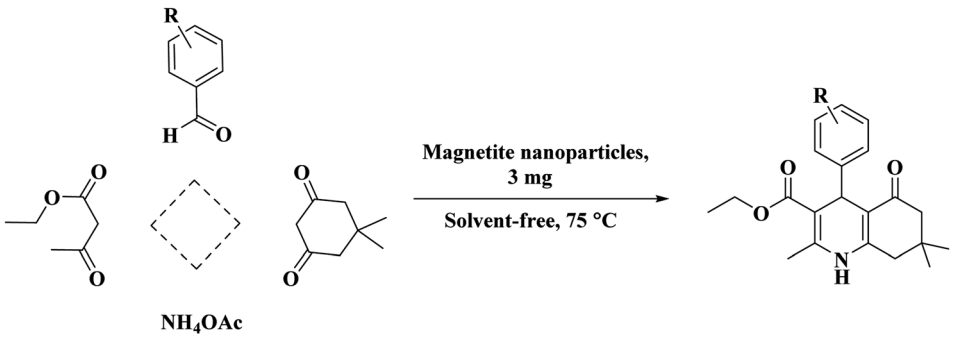

Scheme 1 The preparation of polyhydroquinolines using the PC/Fe_3O_4 nanocomposite.

been used in the process of drug delivery, designing reagents in cancer treatment, and designing absorbent materials to remove inorganic and organic pollutants from the environment.[44–53] Recently, various catalysts such as iron-doped Se/C and magnetic Se/Fe/PCN using carbon and iron elements were designed. These include the iron-doped Se/C applied as heterogeneous catalysts for the selective epoxidation of β-ionone to give 5,6-epoxy-β-ionone,[54] and magnetic Se/Fe/PCN used for the oxidative cracking of styrene derivatives.[55]

Thus, we have applied peanut shells as bio-waste to prepare porous carbon as a template for the placement of ferrous ferric oxide on this media to give porous carbon/Fe_3O_4 nanocomposite (PC/Fe_3O_4 nanocomposite), which was successfully used as an efficient heterogeneous and reusable catalyst for the synthesis of polyhydroquinolines (Scheme 1).

2. Experimental

2.1. Procedure for the synthesis of the PC/Fe_3O_4 nanocomposite

Fe_3O_4 nanoparticles were prepared according to previous literature.[31] Peanut shells were crushed and ground in a mortar, and subsequently burned. Then, the burnt peanut shell (0.075 g) was added to the prepared magnetite nano magnetite (0.025 g), and the mixture was heated in the oven for 4 hours at 600 °C to produce the PC/Fe_3O_4 nanocomposite.

2.2. General procedure for the synthesis of polyhydroquinoline derivatives

To a round-bottomed flask, aryl aldehyde (1 mmol), ethyl acetoacetate (1 mmol, 0.13 g), dimedone (1 mmol, 0.14 g) and ammonium acetate (1 mmol, 0.77 g) were added. The PC/Fe_3O_4 nanocomposite (0.003 g) was added to the round-bottomed flask containing the starting materials and connected to a reflux condenser, and heated at 75 °C under solvent free condition for the appropriate time (Table 2). After the formation of a significant amount of the desired product according to the TLC test using a mixture of *n*-hexane and ethyl acetate solvents with a volume ratio of 1 : 2, the PC/Fe_3O_4 nanocomposite was separated by an external magnet. The corresponding product was then purified by the recrystallization process in ethanol (70%).

2.3. Spectral data of compounds

2.3.1 Ethyl-2,7,7-trimethyl-5-oxo-4-(*p*-tolyl)-1,4,5,6,7,8-hexahydroquinoline-3-carboxylate (2). White solid; M.p.; 259–261 °C; IR (KBr, cm^{-1}): 3276, 3208, 3083, 2935, 1701, 1647, 1605, 1495, 1380, 1215, 1194, 1072 cm^{-1}; ^{1}H NMR (250 MHz, DMSO-d_6): δ (ppm) 0.83 (s, 3H), 0.98 (s, 3H), 1.11 (t, J = 6.75 Hz, 3H), 1.94 (d, J = 16.00 Hz, 2H), 2.17 (s, 3H), 2.22 (s, 3H), 2.36–2.48 (m,

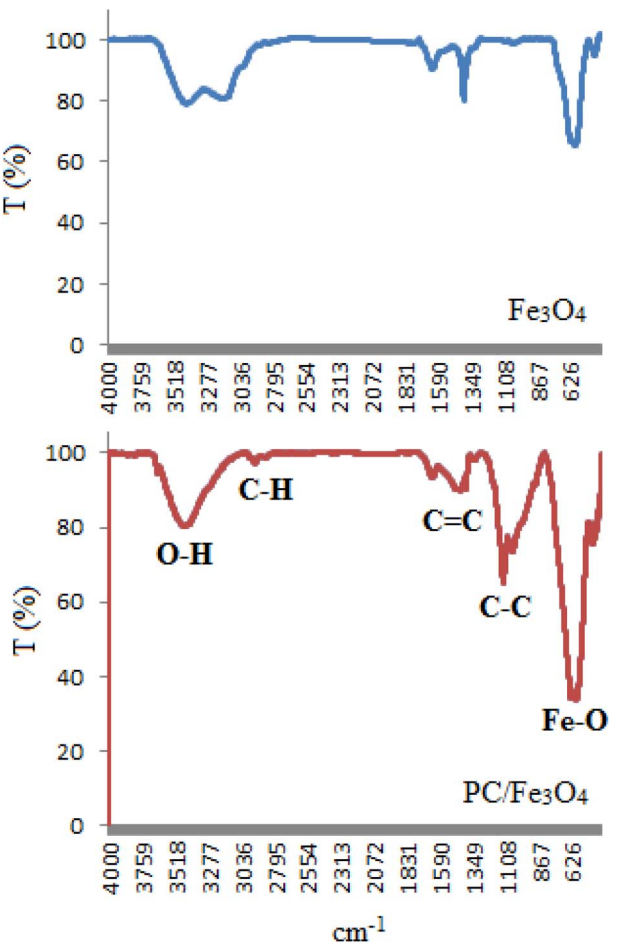

Fig. 1 FT-IR spectrum of the PC/Fe_3O_4 nanocomposite in comparison with Fe_3O_4.

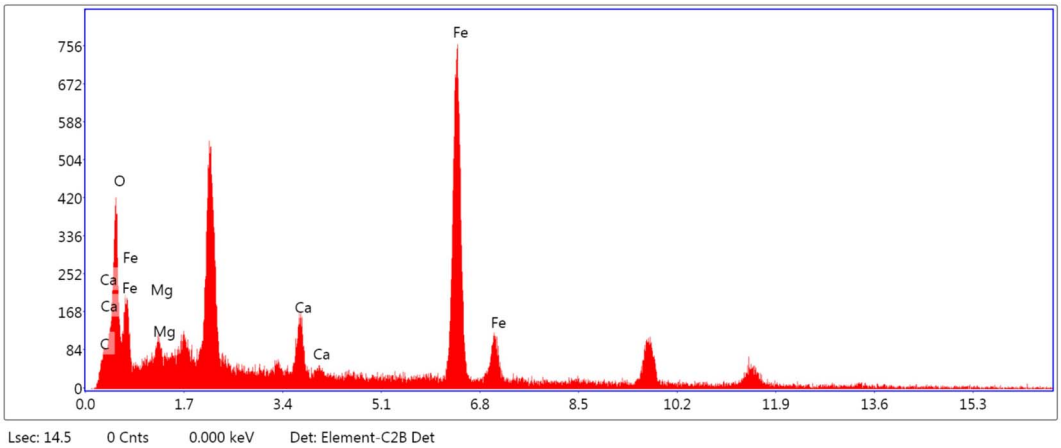

Fig. 2 Energy-dispersive X-ray spectroscopy (EDX) of the PC/Fe_3O_4 nanocomposite.

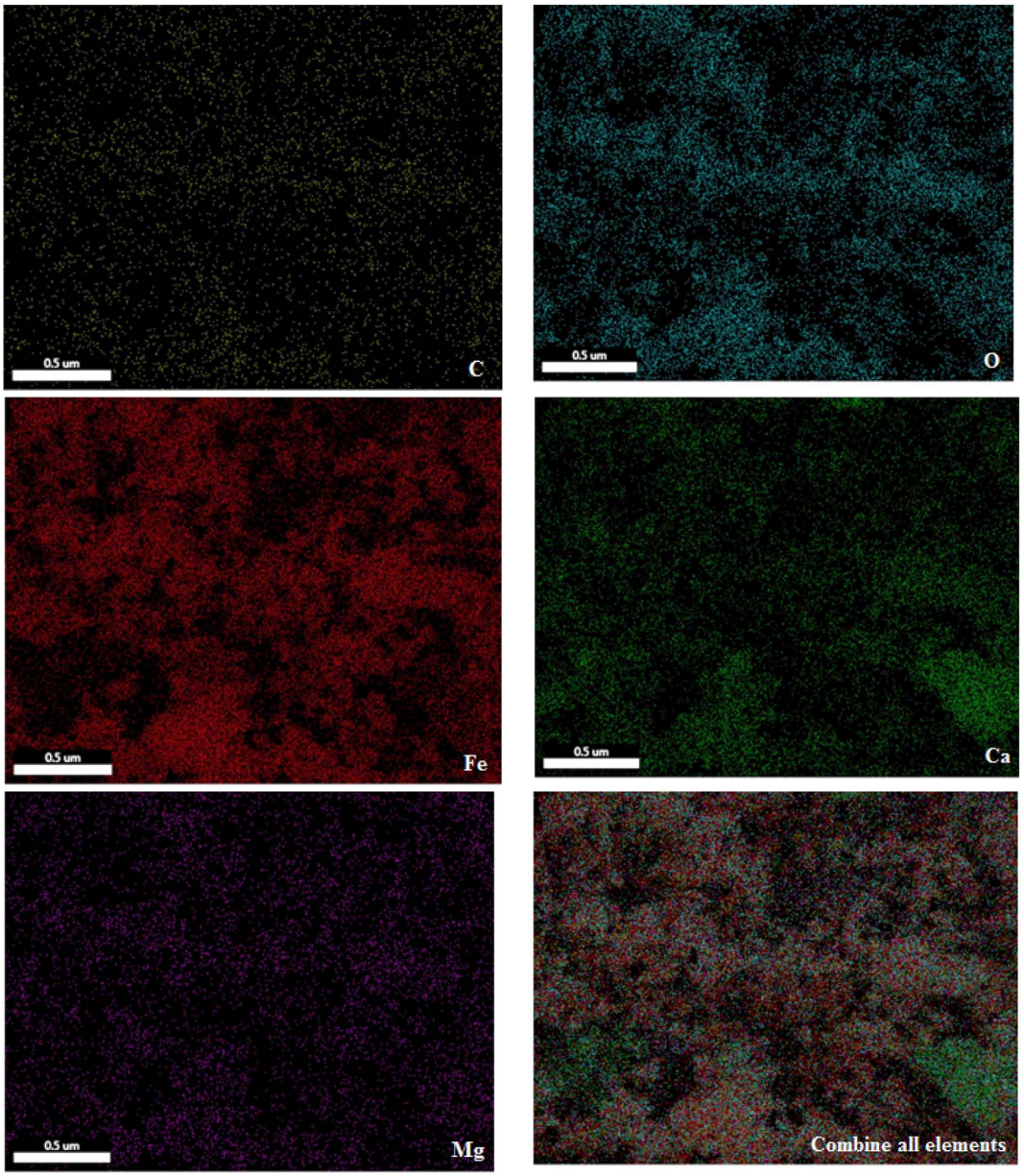

Fig. 3 SEM coupled EDX (SEM mapping) of the PC/Fe_3O_4 nanocomposite.

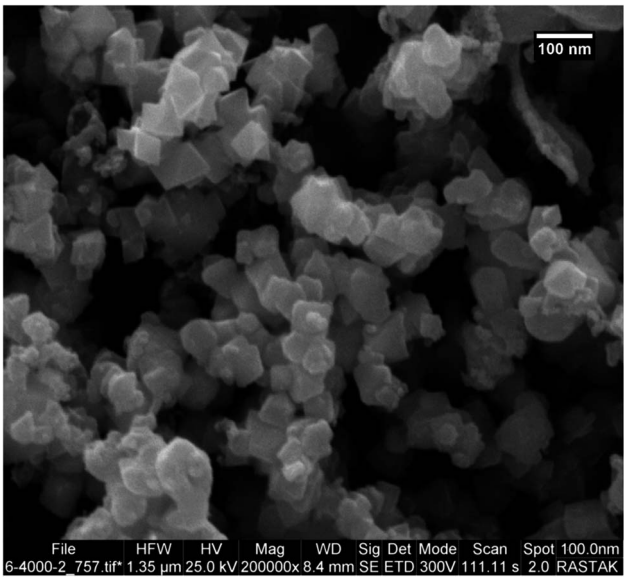

Fig. 4 SEM image of the PC/Fe_3O_4 nanocomposite.

2H), 3.90–3.96 (m, 2H), 4.79 (s, 1H), 6.93–7.02 (m, 4H), 9.01 (s, 1H); ^{13}C NMR (62.5 MHz, DMSO-d_6): δ (ppm) 14.5, 18.6, 20.9, 26.8, 29.5, 32.5, 35.7, 50.6, 59.3, 104.1, 110.4, 127.7, 128.6, 134.9, 145.1, 149.7, 167.2, 194.6.

2.3.2 Ethyl-4-(3-hydroxyphenyl)-2,7,7-trimethyl-5-oxo-1,4,5,6,7,8-hexahydroquinoline-3-carboxylate (5). White solid; M.p.; 229–231 °C; IR (KBr, cm^{-1}): 3279, 3085, 2963, 1688, 1618, 1488, 1215, 1172, 869, 779; ^{1}H NMR (250 MHz, DMSO-d_6): δ (ppm) 0.85 (s, 3H), 0.99 (s, 3H), 1.12 (t, J = 6.75 Hz, 3H), 2.05 (dd, J = 29, 16 Hz, 2H), 2.25 (s, 3H), 2.35–2.48 (m, 2H), 3.40 (d, J = 7.00 Hz, 2H), 4.77 (s, 1H), 6.44 (d, J = 7.50 Hz, 1H), 6.57 (s, 2H), 6.62 (t, J = 7.25 Hz, 1H), 9.01 (s, 1H), 9.07 (s, 1H); ^{13}C NMR (62.5 MHz, DMSO-d_6): δ (ppm) 14.5, 18.6, 26.9, 29.5, 32.4, 35.9, 50.6, 59.4, 104.04, 110.3, 113.01, 114.9, 118.5, 128.8, 145.08, 149.3, 149.8, 157.2, 167.3, 194.6.

2.3.3 Ethyl-4-(2,4-dichlorophenyl)-2,7,7-trimethyl-5-oxo-1,4,5,6,7,8-hexahydroquinoline-3-carboxylate (7). White solid; M.p.; 242–244 °C; IR (KBr, cm^{-1}): 3283, 3078, 2957, 1706, 1647, 1609, 1107, 1073 cm^{-1}; ^{1}H NMR (250 MHz, DMSO-d_6): δ (ppm) 0.81 (s, 3H), 0.97 (s, 3H), 1.05 (t, J = 6.50 Hz, 3H), 2.00

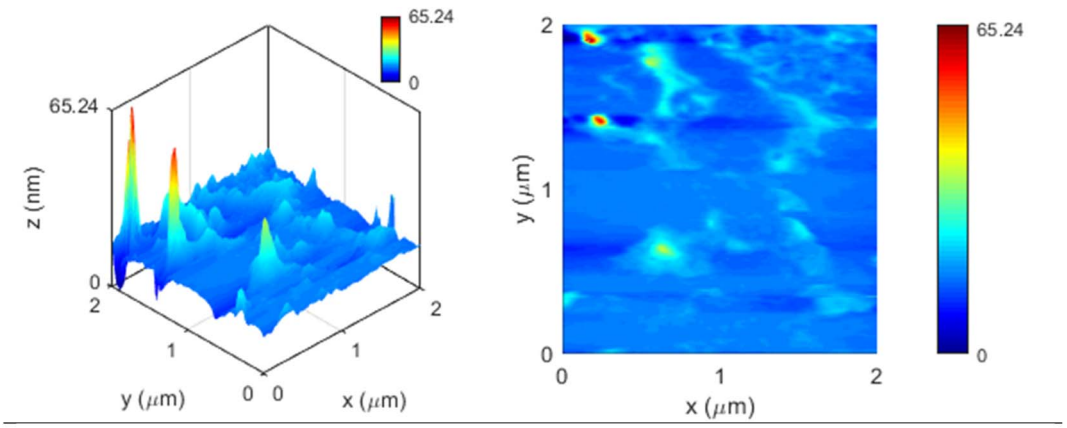

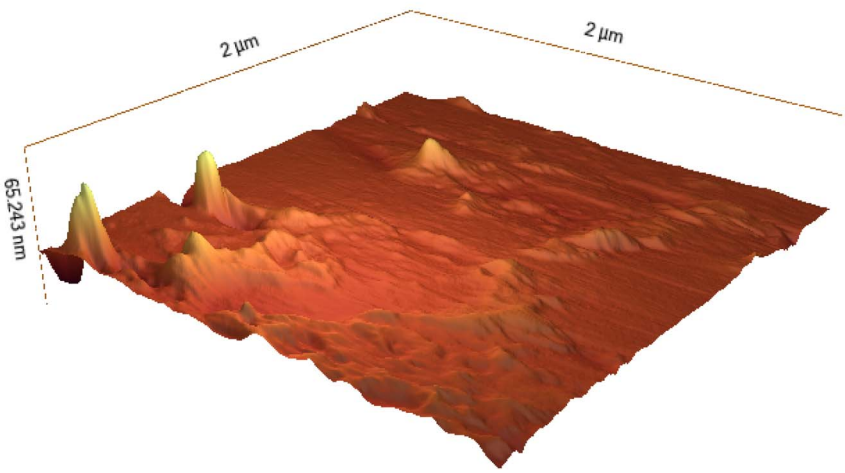

Fig. 5 Atomic force microscopy (AFM) analysis of the PC/Fe_3O_4 nanocomposite.

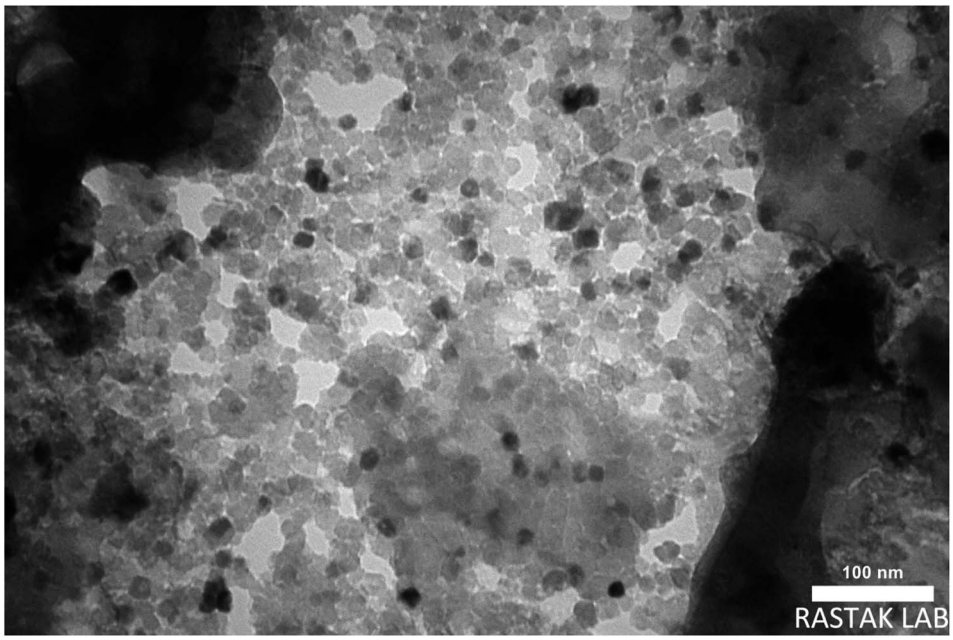

Fig. 6 TEM image of the PC/Fe_3O_4 nanocomposite.

(dd, J = 42, 16 Hz, 2H), 2.23 (s, 3H), 2.36–2.48 (m, 2H), 3.91 (d, J = 6.50 Hz, 2H), 5.12 (s, 1H), 7.25 (s, 2H), 7.32 (s, 1H), 9.13 (s, 1H); ^{13}C NMR (62.5 MHz, DMSO-d_6): δ (ppm) 14.4, 18.6, 26.7, 29.4, 32.3, 35.1, 50.5, 59.4, 103.1, 109.6, 127.2, 128.5, 131.1, 133.2, 144.6, 145.8, 150.2, 166.9, 194.3.

3. Results and discussion

In the presented work, peanut shell was used as a biowaste source for the preparation of porous carbon. Accordingly, the peanut shells were crushed and burned. In the next step, the crushed burnt peanut shells were mixed with magnetite nanoparticles with a mass ratio of 3 : 1. The obtained mixture was well-ground and then heated at 600 °C for 4 hours to give a porous carbon/Fe_3O_4 nanocomposite (PC/Fe_3O_4 nanocomposite). The magnetite nanocomposite was produced from the pyrolysis process containing iron oxide magnetic nanoparticles in porous carbon with high active surface, which can be used as an efficient and recyclable catalyst for the synthesis of organic compounds. The structure of the PC/Fe_3O_4 nanocomposite was studied by FT-IR, EDX, SEM mapping, SEM, AFM, TEM, and VSM analyses, and then its catalytic ability was investigated for the synthesis of polyhydroquinolines.

To identify the PC/Fe_3O_4 nanocomposite, the FT-IR spectrum of the composite particles was first studied to find the different kinds of various bonds (Fig. 1). A broad peak that appeared at 3200–3600 cm^{-1} could be related to the O–H bonds from the hydroxyl groups. Other peaks at 1634 and 1111 cm^{-1} corresponded to the C=C and C–C bond vibrations of the carbon skeleton, respectively. The peak at about 624 cm^{-1} is also related to the Fe–O bond vibration. The FT-IR spectrum of the PC/Fe_3O_4 nanocomposite in comparison with that of Fe_3O_4 is given in Fig. 1.

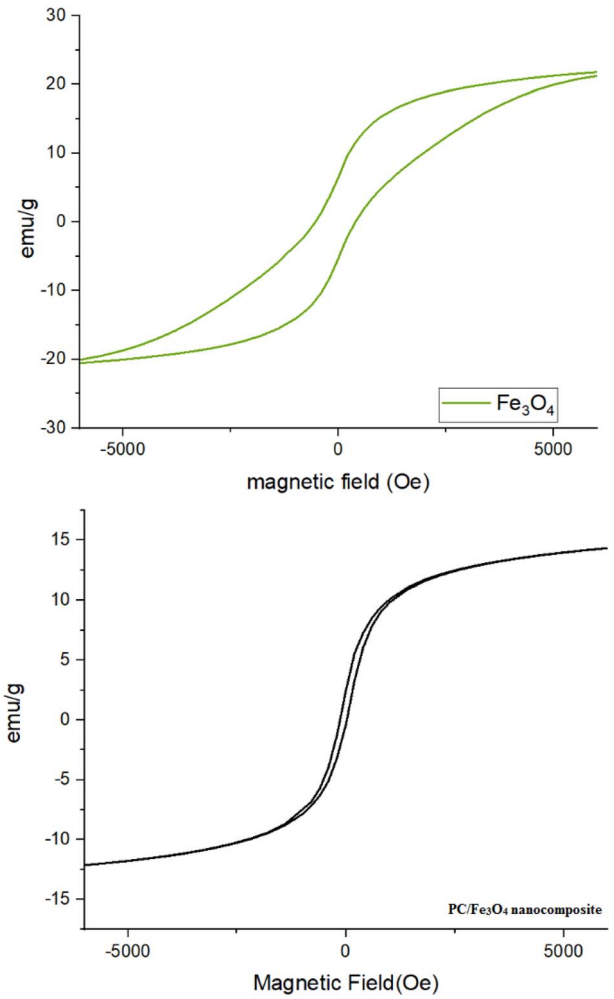

Fig. 7 Vibrating sample magnetometer (VSM) analysis of the PC/Fe_3O_4 nanocomposite compared with Fe_3O_4.

After the determination of various bonds in the magnetite nanocomposite structure, the kind of elements was studied by energy-dispersive X-ray spectroscopy (EDX) (Fig. 2). According that, the expected elements such as carbon, oxygen, iron were observed in this structure. Moreover, calcium and magnesium were also beholden in this structure.

To show the kind of elements and distribution of them in the structure of catalyst, SEM coupled EDX (SEM mapping) of PC/Fe_3O_4 nanocomposite was investigated. As seen in Fig. 3, elements including iron, oxygen, carbon, calcium and magnesium are well distributed in the magnetic nanocomposite structure.

To determine the morphology and particle size of the magnetite nanocomposite, the size of the prepared nanoparticles was investigated by scanning electron microscopy (SEM) (Fig. 4). As seen in Fig. 4, the obtained particles of the PC/Fe_3O_4 nanocomposite were prepared in a size less than 100 nm.

Atomic Force Microscopy (AFM) analysis is a useful technique for nanoparticle measurement. Using surface topographies and atomic force measurement, the nanoparticle size determination and particle distribution were investigated. In this test, the nanoparticle was imaged in two-dimensional and three-dimensional surface topographies, and two sizes at 2 and 10 microns. In the two-micron test, the two-dimensional and three-dimensional topographies of the nanoparticle at a size of 65 nm was observed in the surface topography, similar to the other tests performed. The color change from blue to red indicates the increase in particle size (Fig. 5).

The size of the prepared magnetite nanocomposite was also studied by transmission electron microscopy (TEM). As shown in Fig. 6, the magnetite nanocomposite particles were produced in an orderly manner with dimensions of less than 100 nm. The preparation of the magnetite nanocomposite at the nano-scale increased the active surface and improved its catalytic ability.

Table 1 The optimization of the reaction condition on the model reaction

Entry	Solvent	Catalyst amount (mg)	Temp. (°C)	Time (min)	Yield[a] (%)
1	—	2	75	6	71
2	—	3	75	6	95
3	—	4	75	6	91
4	—	3	95	6	88
5	—	3	50	6	73
6	Ethyl acetate	3	Reflux	6	64
7	$CHCl_3$	3	Reflux	6	79
8	EtOH	3	Reflux	6	95
9	*n*-Hexane	3	Reflux	6	30
10	THF	3	Reflux	6	19
11	CH_2Cl_2	3	Reflux	6	20

[a] Isolated yield.

Table 2 The preparation of polyhydroquinolines

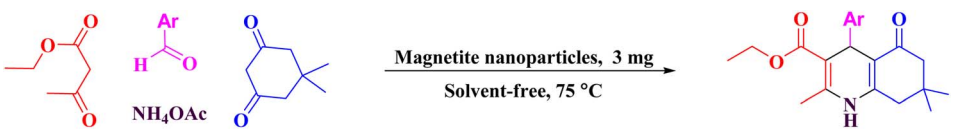

Product no.	Ar	Time (min)	Yield[a] (%)	M.p. (°C) [lit.]
1	C_6H_5	6	95	220–222 (218–221)[56]
2	4-$CH_3C_6H_4$	19	84	259–261 (262–263)[18]
3	4-$CH_3OC_6H_4$	19	89	248–252 (256–258)[18]
4	2-FC_6H_4	10	91	223–226 (229–231)[56]
5	3-OHC_6H_4	16	81	229–231 (226–229)[56]
6	2-ClC_6H_4	13	94	199–203 (205–207)[57]
7	2,4-diClC_6H_3	10	92	242–244 (244–245)[18]
8	2,5-di$CH_3OC_6H_3$	10	88	210–212 (215–217)[58]
9	2,6-diClC_6H_3	15	90	257–259 (263–265)[59]
10	3,4-di$CH_3OC_6H_3$	12	85	209–214 (202–204)[30]
11	3-ClC_6H_4	9	96	210–214 (206–207)[60]
12	3-OH,4-$CH_3OC_6H_4$	20	90	211–214 (209–211)[7]
13	3-FC_6H_4	8	92	206–208 (206–208)[61]
14	3,4,5-tri$CH_3OC_6H_2$	22	87	197–202 (193–195)[62]

[a] Isolated product.

The magnetic behavior of the magnetite nanocomposite was measured using a vibrating sample magnetometer (VSM) at room temperature, and compared with that of Fe_3O_4 (Fig. 7). The saturation magnetization for the PC/Fe_3O_4 nanocomposite was found to be 12 emu g^{-1} (Fig. 7). The magnetic ability of this nanocomposite makes it possible for recovery from the reaction mixture and makes it easily reusable.

After the characterization of the porous carbon/Fe_3O_4 nanocomposite (PC/Fe_3O_4 nanocomposite) by various analyses, the catalytic application of the PC/Fe_3O_4 nanocomposite on the synthesis of polyhydroquinolines was investigated. For this purpose, the reaction of benzaldehyde with dimedone, ethyl acetoacetate and ammonium acetate was selected as a model reaction, and the effect of different factors on this reaction was studied. After that, the effect of different temperatures, different amounts of magnetic catalyst, and various solvents on the model reaction were studied. In another step, the model reaction was also investigated in the absence of solvent (Table 1). Based on Table 1, it is concluded that a high yield of product and a short reaction time were obtained in the presence of 3 mg of PC/Fe_3O_4 nanocomposite at 75 °C under solvent-free conditions. Various solvents, such as ethyl acetate, $CHCl_3$, CH_2Cl_2,

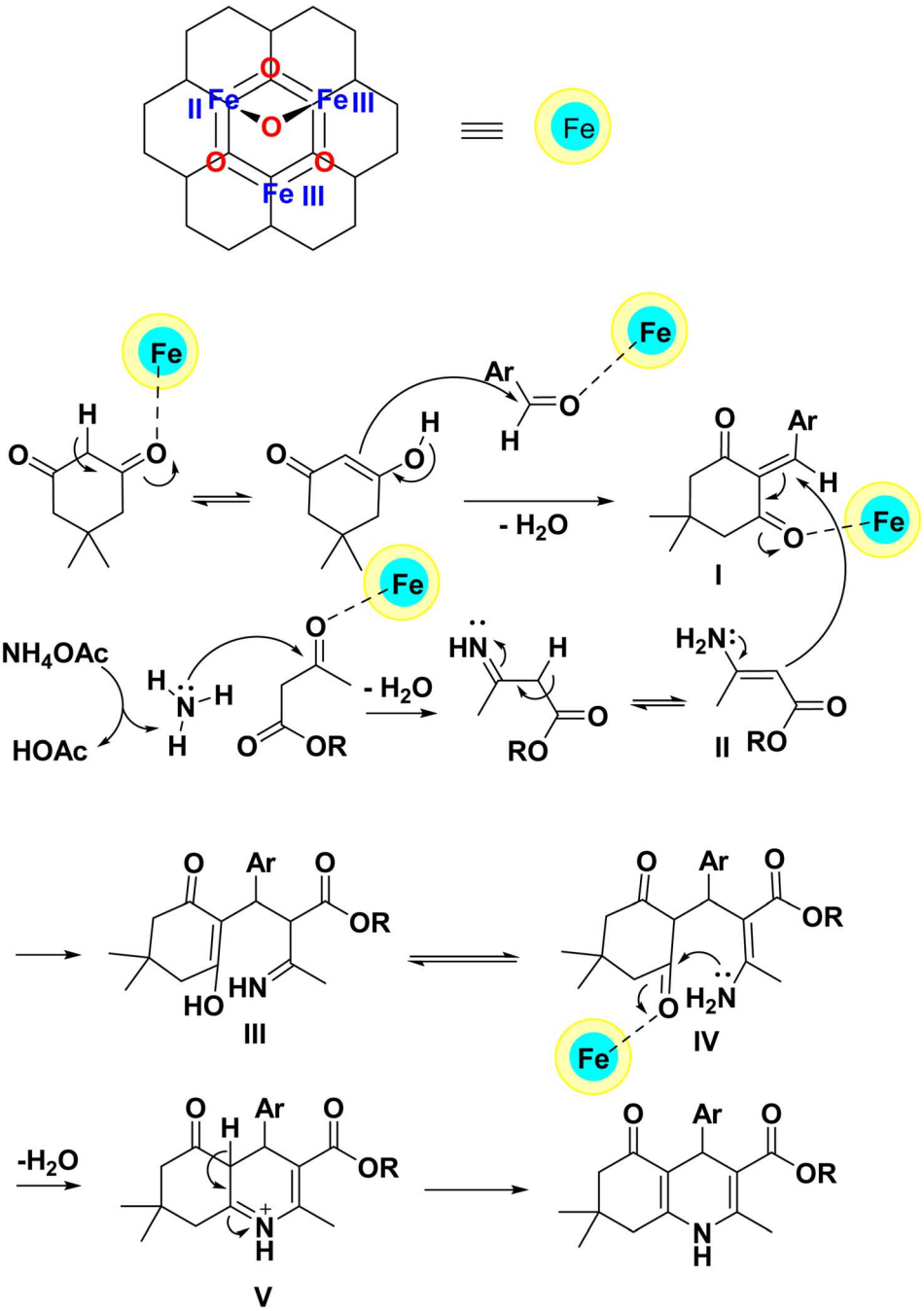

Scheme 2 The proposed mechanism for the preparation of polyhydroquinolines using the PC/Fe_3O_4 nanocomposite.

EtOH, THF, and *n*-hexane, were tested in this reaction, wherein the effect of EtOH as a solvent is similar to solvent-free conditions. However, due to saving the solvent and materials, it is preferred to carry out the reaction in the absence of solvent. Accordingly, the use of 3 mg of PC/Fe_3O_4 nanocomposite as a catalyst at 75 °C under solvent-free condition was chosen as an optimal reaction condition for the synthesis of polyhydroquinolines.

To investigate the synergistic effect of peanut shell and iron oxide magnetite nanoparticles on each other, the model reaction was performed with each of these components as the catalyst alone, and the related product yield was 36% after 30 minutes and 81% after 30 minutes, respectively. Neither component had the ability to be the main catalyst for this reaction. Furthermore, this reaction was investigated in the absence of a catalyst at 75 °C under solvent-free condition, which produced a product yield of 28% after 17 minutes.

After the optimization of the reaction conditions, various aryl aldehydes containing electron-withdrawing groups, electron-donating groups and halogens on their ring were tested in this reaction to find the generality and efficiency of the presented method on the synthesis of polyhydroquinolines (Table 2). As shown in Table 2, the expected products were prepared in high yields and suitable reaction times. Spectral data of some products are given in ESI (Fig. S2–S10†).

According to previous reports in the synthesis of polyhydroquinoline compounds,[18,56–62] dimedone is converted into an enol structure after activation by the PC/Fe_3O_4 nanocomposite. In this form, it reacts with the aldehyde activated by the catalyst to produce intermediate (I). In the other part of the reaction, ethyl acetoacetate reacts with ammonia produced from ammonium acetate and produces enamine (II). After this step, intermediates (I) and (II) react with each other to produce intermediate (III). Intermediate (III) is transformed into intermediate (IV) by tautomerization. Furthermore, while performing an intramolecular nucleophilic attack of the NH_2 group on the carbonyl group and removing a water molecule, it produces intermediate (V). As a result, the polyhydroquinoline derivative is produced after tautomerization in intermediate (V) (Scheme 2).

One of the important advantages of the PC/Fe_3O_4 nanocomposite is its magnetic property, which results in its easy separation from the reaction mixture. Accordingly, the reusability of the catalyst was studied using the model reaction. The reaction of benzaldehyde with dimedone, ethyl acetoacetate and ammonium acetate was carried out in the presence of the PC/Fe_3O_4 nanocomposite (3 mg) at 75 °C. After the completion of the reaction, the catalyst was collected by an external magnet and separated from the reaction mixture. The recovered catalyst was washed with warm ethanol and used in another reaction after drying. The recovered PC/Fe_3O_4 nanocomposite was well used in three other experiments, and the corresponding product was produced with significant efficiency (Fig. 8).

To show the changes in the magnetization of the reused catalyst in comparison with a fresh catalyst, their magnetic behaviors were measured using a vibrating sample magnetometer (VSM) at room temperature (Fig. 9). According to Fig. 9, there are not many changes observed in the magnetic ability of the reused catalyst after reaction catalysis.

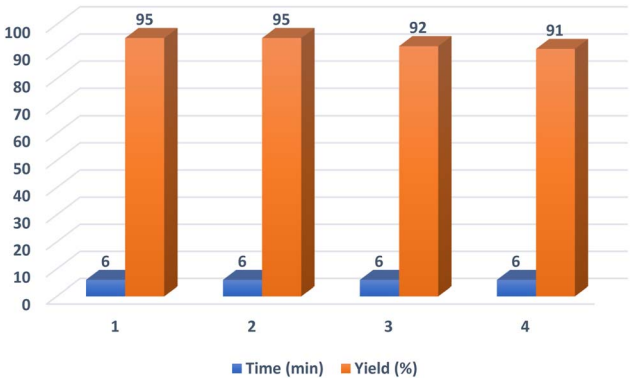

Fig. 8 The reusability of the PC/Fe_3O_4 nanocomposite.

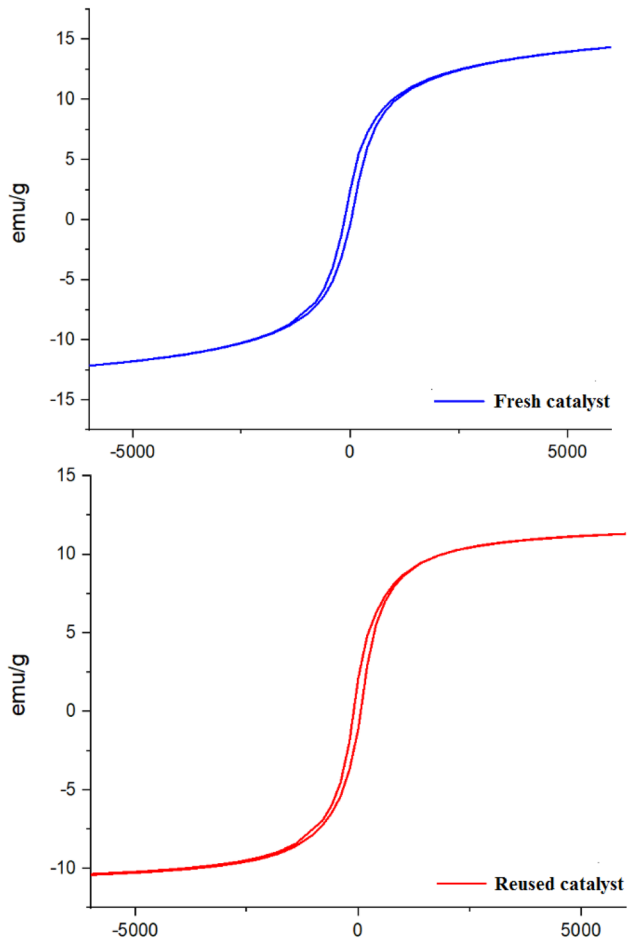

Fig. 9 Vibrating sample magnetometer (VSM) analysis of the reused catalyst compared with a fresh catalyst.

4. Conclusions

In conclusion, the porous carbon/Fe_3O_4 nanocomposite (PC/Fe_3O_4 nanocomposite) was prepared by the pyrolysis of peanut shells as a bio-waste material with magnetite nanoparticles. The

structure of the PC/Fe_3O_4 nanocomposite was studied by FT-IR, EDX, SEM mapping, SEM, AFM, TEM, and VSM analyses. The catalytic ability of the PC/Fe_3O_4 nanocomposite as a reusable and heterogeneous catalyst was successfully tested on the preparation of hexahydroquinoline derivatives by the reaction of various aryl aldehydes, ethyl acetoacetate, dimedone and ammonium acetate.

Data availability

The datasets supporting this article have been uploaded as part of the ESI.†

Conflicts of interest

There are no conflicts to declare.

References

1 R. Simsek, U. B. Ismailoglu, C. Safak and I. Sahin-Erdemli, *Farmaco*, 2000, **55**, 665.
2 R. D. Larsen, E. G. Corley, A. O. King, J. D. Carrol, P. Davis, T. R. Verhoeven, P. J. Reider, M. Labelle, J. Y. Gauthier, Y. B. Xiang and R. Zamboni, *J. Org. Chem.*, 1996, **61**, 3398.
3 Y. L. Chen, K. C. Fang, J. Y. Sheu, S. L. Hsu and C. C. Tzeng, *J. Med. Chem.*, 2001, **44**, 2374.
4 G. Roma, M. D. Braccio, G. Grossi and M. Chia, *Eur. J. Med. Chem.*, 2000, **35**, 1021.
5 D. Doube, M. Bloun, C. Brideau, C. Chan, S. Desmarais, D. Eithier, J. P. Falgueyeret, R. W. Friesen, M. Girad, Y. Girad, J. Guay, P. Tagari and R. N. Yong, *Bioorg. Med. Chem. Lett.*, 1998, **8**, 1225.
6 M. P. Maguire, K. R. Sheets, K. Mcvety, A. P. Spada and A. Ziberstein, *J. Med. Chem.*, 1994, **37**, 2129.
7 P. N. Kalaria, S. P. Satasia and D. K. Raval, *Eur. J. Med. Chem.*, 2014, **78**, 207.
8 R. Taghavi and S. Rostamnia, *Chem. Methodol.*, 2022, **6**, 639.
9 Z. A. K. Al-Messri, *Chem. Methodol.*, 2023, **7**, 581.
10 M. Farajpour, S. M. Vahdat, S. M. Baghbanian and M. Hatami, *Chem. Methodol.*, 2023, **7**, 540.
11 R. M. Muhiebes, L. Fatolahi and S. Sajjadifar, *Asian J. Green Chem.*, 2023, **7**, 121.
12 Y. Ghalandarzehi and H. Kord-Tamandani, *Asian J. Green Chem.*, 2023, **7**, 70.
13 M. A. Amiri, H. Younesi, H. K. Aqmashhadi, G. F. Pasha, S. Asghari and M. Tajbakhsh, *Chem. Methodol.*, 2024, **8**, 1.
14 R. M. Mhaibes, Z. Arzehgar, M. M. Heydari and L. Fatolahi, *Asian J. Green Chem.*, 2023, **7**, 1.
15 H. Ghafuri, M. Zargari and A. Emami, *Asian J. Green Chem.*, 2023, **7**, 54.
16 A. R. Moosavi-Zare, H. Goudarziafshar, Z. Jalilian and F. Hosseinabadi, *Chem. Methodol.*, 2022, **6**, 571.
17 A. R. Moosavi-Zare, Z. Asgari, A. Zare, M. A. Zolfigol and M. Shekouhy, *RSC Adv.*, 2014, **4**, 60636.
18 A. Khazaei, A. R. Moosavi-Zare, H. Afshar-Hezarkhani and V. Khakyzadeh, *RSC Adv.*, 2014, **4**, 32142.
19 A. Khazaei, M. A. Zolfigol and A. R. Moosavi-Zare, *Chin. J. Catal.*, 2013, **34**, 1936.
20 A. R. Moosavi-Zare, H. Goudarziafshar and L. Ghaffari, *Appl. Organomet. Chem.*, 2017, **31**, e3845.
21 A. R. Moosavi-Zare, M. A. Zolfigol, M. Zarei, A. Zare and J. Afsar, *Appl. Catal., A*, 2015, **505**, 224.
22 H. Goudarziafshar, A. R. Moosavi-Zare, K. Saki and M. Abdolmaleki, *J. Chin. Chem. Soc.*, 2017, **64**, 1496.
23 A. Khazaei, L. Jafari-Ghalebabakhani, E. Ghaderi, M. Tavasoli and A. R. Moosavi-Zare, *Appl. Organomet. Chem.*, 2017, **31**, e3815.
24 A. Khazaei, M. Tavasoli, V. Jamshidi, F. G. Ghalil and A. R. Moosavi-Zare, *Appl. Organomet. Chem.*, 2018, **32**, e4368.
25 S. Esmaili, A. Khazaei, A. Ghorbani-Choghamarani and M. Mohammadi, *RSC Adv.*, 2022, **12**, 14397.
26 A. R. Moosavi-Zare and H. Afshar-Hezarkhani, *Eurasian Chem. Commun.*, 2020, **2**, 465.
27 A. Gorji, T. Akbarpour and A. Khazaei, *Polycyclic Aromat. Compd.*, 2022, **43**, 5041.
28 S. B. Sapkal, K. F. Shelke, B. B. Shingate and M. S. Shingare, *Tetrahedron Lett.*, 2009, **15**, 1754.
29 M. Ghorbani, H. R. Shaterian, S. Noura, F. Khammar, K. Behbodi, B. Reisi and M. Oftadeh, *J. Mol. Liq.*, 2015, **204**, 15.
30 R. Surasani, D. Kalita, A. V. D. Rao, K. Yarbagi and K. B. Gandrasekhar, *J. Fluorine Chem.*, 2012, **135**, 91.
31 A. Gorji, S. Esmaili, A. R. Moosavi-Zare and A. Khazaei, *J. Mol. Struct.*, 2024, **1314**, 138797.
32 X. B. Lu and D. J. Darensbourg, *Chem. Soc. Rev.*, 2012, **41**, 1462.
33 C. Wang, J. Kim, J. Tang, J. Na, Y.-M. Kang, M. Kim, H. Lim, Y. Bando, J. Li and Y. Yamauchi, *Angew. Chem., Int. Ed.*, 2020, **59**, 2066.
34 G. Singh, K. S. Lakhi, S. Sil, S. V. Bhosale, I. Kim, K. Albahily and A. Vinu, *Carbon*, 2019, **148**, 164.
35 Y. Chen, X. Zhang, W. Chen, H. Yang and H. Chen, *Bioresour. Technol.*, 2017, **246**, 101.
36 Y. Li, G. Wang, T. Wei, Z. Fan and P. Yan, *Nano Energy*, 2016, **19**, 165.
37 X. Chen, S. Song, H. Li, G. Gözaydın and N. Yan, *Acc. Chem. Res.*, 2021, **54**, 1711.
38 K. Lee, Y. Jing, Y. Wang and N. Yan, *Nat. Rev. Chem.*, 2022, **6**, 635.
39 M. Ding, X. Liu and J. Yao, *New J. Chem.*, 2021, **45**, 4147.
40 Q. An, C. Liu, S. Deng, Y. Jiao, M. Tang, M. Yang, Z. Ye and B. Zhao, *Chemosphere*, 2022, **304**, 135308.
41 M. Cao, C. Long, S. Sun, Y. Zhao, J. Luo and D. Wu, *J. Energy Inst.*, 2021, **96**, 90.
42 Z. Jalilian, A. R. Moosavi-Zare, M. Ghadermazi and H. Goudarziafshar, *RSC Adv.*, 2023, **13**, 10642.
43 K.-L. Chang, S. C. Muega, B. I. G. Ofrasio, W.-H. Chen, E. G. Barte, R. R. M. Abarca and M. D. G. de Luna, *Chemosphere*, 2022, **291**, 132829.
44 M. A. Zolfigol, V. Khakyzadeh, A. R. Moosavi-Zare, A. Rostami, A. Zare, N. Iranpoor, M. H. Beyzavi and R. Luque, *Green Chem.*, 2013, **15**, 2132.

45 L. M. Rossi, N. J. S. Costa, F. P. Silva and R. Wojcieszak, *Green Chem.*, 2014, **16**, 2906.
46 F. Hakimi, A. Sharifi-Zarchi and E. Golrasan, *Chem. Methodol.*, 2023, **7**, 489.
47 S. Ghasemi, F. Badri and H. R. Kafshboran, *Asian J. Green Chem.*, 2024, **8**, 39.
48 N. Pourbahar and S. S. Alamdar, *Asian J. Green Chem.*, 2023, **7**, 9.
49 E. Ezzatzadeh, *J. Med. Nanomater. Chem.*, 2023, **5**, 213.
50 X. Li, H. Zhou, R. Qian, X. Zhang and L. Yu, *Chin. Chem. Lett.*, 2024, **22**, 110036.
51 X.-Q. Li, S. Feng, J. Yang, T.-P. Xie, J.-K. Wang, X.-J. Chen, D.-S. Kong and H.-Y. Chen, *Rare Met.*, 2023, **42**, 862.
52 A. R. Moosavi-Zare, R. Najafi and H. Goudarziafshar, *RSC Adv.*, 2024, **14**, 19167.
53 S. Esmaili, A. R. Moosavi-Zare and A. Khazaei, *RSC Adv.*, 2022, **12**, 5386.
54 H. Cao, P. Li, X. Jing and H. Zhou, *Chin. J. Org. Chem.*, 2022, **42**, 3890.
55 Z. Wenjian, X. Xinrui, L. Yonghong and Z. Xu, *Chin. J. Org. Chem.*, 2022, **42**, 1849.
56 S. A. Salem, A. Khazaei, J. Y. Seyf, N. Sarmasti and M. M. Gilan, *Polycyclic Aromat. Compd.*, 2021, **41**, 319.
57 A. Khazaei, N. Sarmasti, J. Yousefi Seyf and M. Tavasoli, *RSC Adv.*, 2015, **5**, 101268.
58 F. Mirzaei, H. Valizadeh and M. Pazhang, *J. Iran. Chem. Soc.*, 2024, **21**, 639.
59 S.-J. Song, Z.-X. Shan and Y. Jin, *Synth. Commun.*, 2010, **40**, 3067.
60 B. Sakram, B. Sonyanaik, K. Ashok and S. Rambabu, *Res. Chem. Intermed.*, 2016, **42**, 7651.
61 S. Zhaleh, N. Hazeri, M. R. Faghihi and M. T. Maghsoodlou, *Res. Chem. Intermed.*, 2016, **42**, 8069.
62 M. Tajbakhsh, H. Alinezhad, M. Norouzi, S. Baghery and M. Akbari, *J. Mol. Liq.*, 2013, **177**, 44.